

## Role of nuclear dynamics in deducing the fusion-fission time scales from prescission neutron multiplicities

K. Siwek-Wilczyńska

*Institute of Experimental Physics, Warsaw University, 00-681 Warsaw, Poland*

J. Wilczyński

*Soltan Institute for Nuclear Studies, 05-400 Otwock-Swierk, Poland*

R. H. Siemssen and H. W. Wilschut

*Kernfysisch Versneller Instituut, 9747 AA Groningen, The Netherlands*

(Received 7 November 1994)

Existing data on the prescission neutron multiplicities have been analyzed with a new method combining time-dependent statistical cascade calculations with Feldmeier's model of the dynamics of nucleus-nucleus collisions. The analysis resulted in the determination of the time scale  $\tau_f$  of fusion-fission reactions for different composite systems with excitation energies ranging from 80 to 240 MeV. The deduced values of  $\tau_f$  range from  $5 \times 10^{-20}$  to  $10^{-18}$  s. These time scales are approximately 10 times longer than those deduced for the same set of data with the "static" model used by Hinde and collaborators.

PACS number(s): 25.70.Jj

### I. INTRODUCTION

It was shown in a series of papers (see, e.g., [1–5], and references therein) that triple coincidence measurements involving two fission fragments and a neutron give the possibility to decompose measured neutron multiplicities into two parts corresponding to the emission before and after scission. In the case of alpha-particle emission, one can get even more detailed information because, in addition to the prescission and postscission multiplicities, the near-scission component can also be extracted [6–9].

The measured prescission and postscission neutron multiplicities were used by Hinde *et al.* [4, 5] as a clock for the time scales of fusion-fission reactions. In turn, data on the prescission and near-scission alpha-particle multiplicities have recently been used [8] for an estimate of the time scale of fission in its final stage and hence for checking the strength of the energy-dissipation mechanism. In addition to the particle evaporation processes, the  $\gamma$  decay of the giant dipole resonance (GDR) was also used [10] for the determination of the time scale of fission.

Presently there already exists an ample collection of data on prescission and postscission multiplicities [4]. Hinde and collaborators have analyzed the whole collection of data by carrying out time-dependent statistical-model calculations in which the cumulative time, corresponding to the measured prescission neutron multiplicity, was interpreted as the duration  $\tau_f$  of the fusion-fission process. It was concluded from the analysis [4] that for all studied reactions the  $\tau_f$  ranges from  $2 \times 10^{-20}$  to  $6 \times 10^{-20}$  s (see Fig. 25 of Ref. [4]).

The analysis of Hinde *et al.* [4] was done in an essentially "static" approximation, in which the initial excitation energy of the composite system was assumed to be available instantly at the time  $t = 0$ , and from that mo-

ment on the deexcitation cascade was calculated as for a standard "static" compound nucleus.

In this paper we present results of our calculations in which time-dependent statistical model calculations were coupled to a dynamical evolution of the intrinsic excitation of the composite system as predicted by the one-body dissipation model of Feldmeier [11, 12]. Several aspects of the interpretation of the prescission neutron multiplicity data are discussed. It is shown that by taking the dynamics of the composite system into account one arrives at much longer times  $\tau_f$  than those deduced by Hinde and collaborators with the static model.

### II. MODEL CALCULATIONS

#### A. General concept

Fusion-fission reactions are dynamic processes of high complexity. The fact that as many as 6–8 neutrons can be evaporated from the hot and heavy composite system prior to fission [4] clearly demonstrates that the fission of these nuclei requires time for the necessary rearrangement in the shape degrees of freedom. With the increasing excitation energy, the mean lifetime that determines the rate of evaporation of light particles becomes so short that fission and evaporation can no longer be viewed as processes competing in terms of the conventional Bohr-Wheeler model [13]. Since the available phase space dictates fission practically in all events ( $\Gamma_n/\Gamma_f \approx 0$ ), one can assume that fission is decided for each event already at  $t = 0$ . Thus in this approach the evaporation cascade takes place *during* the fission process because the composite system is already *destined* to fission ( $P_f = 1$ ).

The concept formulated above is especially appropriate

and useful in attempts to use the measured prescission neutron multiplicities as a “neutron clock” [4, 5] for the determination of the time scale of fusion-fission reactions. It should be emphasized here that all the existing experimental data on the prescission neutron multiplicities have been obtained in the measurements triggered by fission fragments. Therefore in all the events the composite system was indeed destined to fission ( $P_f = 1$ ). Therefore, it is legitimate in this approach to interpret the cumulative time of the prescission cascade as the duration of the fusion-fission process from the formation of the composite system until scission.

An alternative way to determine the time scale of fusion-fission reactions was proposed by Paul and Thoennessen [10]. In their approach the fission width is strongly reduced (relative to the Bohr-Wheeler width) due to a large value of the dissipation constant entering the Kramers factor [14]. The suppression of the fission width combined with the assumed time-dependent building up of the fission flux leads effectively to a delay of fission. This delay time (deduced in Ref. [10] from an analysis of the prescission GDR  $\gamma$ -ray multiplicities) essentially should correspond to the fusion-scission time deduced using our concept of evaporation *during* the fission process (for events for which fission is already determined at the beginning of the time scale,  $P_f = 1$  at  $t = 0$ ).

In addition to the delicate question of the competition between fission and evaporation, we should note that—due to the high angular momenta and the large energies associated with the collective degrees of freedom—the initial conditions characterizing the composite system are not well defined in fusion-fission reactions at high excitation energies. Therefore the traditional concept of a fully equilibrated compound nucleus with a fixed excitation energy appears to be an unrealistic idealization in these reactions.

These reservations have to be kept in mind in estimating the time scales of the fusion-fission reactions. The existing data on prescission neutron multiplicities [4] have been determined for reactions with heavy-ion beams well above the Coulomb barrier. As will be shown in Sec. II C, many partial waves lead in these reactions to a dynamically evolving “mononucleus” that eventually undergoes a fissionlike binary reseparation. As a rule, only for the lowest partial waves, the colliding system gets trapped in the minimum of the potential energy surface behind the saddle. So, only for those nearly central collisions can a “true” compound nucleus be formed. For other collisions at larger angular momenta (that obviously dominate the cross section) the observed fissionlike reactions have to be related to processes that are not completely equilibrated, called quasifission or fast-fission.

In light of these comments, we deduce the time scales of the fusion-fission reactions from the prescission neutron data in the following way: First, the dynamical trajectories are calculated with the Feldmeier’s program HICOL [12] for the whole range of partial waves contributing to the reaction cross section for a given reaction of known prescission neutron multiplicity. From these calculations information is obtained on which trajectories lead to true fusion (when the system is trapped and the compound

nucleus is formed), which trajectories lead to a dynamically evolving composite system that eventually splits into two comparable fragments, i.e., undergoes symmetric “fast-fission,” and finally, which trajectories lead to relatively peripheral reactions without the formation of a “mononucleus.” For all calculated trajectories the program predicts the excitation energy generated (due to the one-body dissipation mechanism) and accumulated in the composite system until a given point of the trajectory.

Our statistical-model code (see Sec. II B) has been constructed in such a way that the excitation energy generated in the composite system, and known at a given time from the HICOL calculation is coupled with the evaporation cascade calculation and thus can modify the actual excitation energy at a given instant of time. This differential modification of the excitation energy is repeated step by step at each stage of the statistical decay sequence.

Note, however, that in our scheme of calculations the dynamics of the colliding system is decoupled from the deexcitation cascade. Fortunately, this simplification is well justified by the fact that, to first order, the one-body dissipation as well as inertia and other parameters determining the dynamics do not depend on the excitation energy or temperature of the system.

Obviously, the amount of thermal excitation energy generated in the colliding system strongly depends on the impact parameter. Therefore the time-dependent statistical-model calculation has to be done individually for some representative values of the angular momentum. The time after which the calculated cumulative number of emitted neutrons is equal to the measured prescission neutron multiplicity is interpreted as the fusion-fission time  $\tau_f$ .

## B. Statistical model calculations

For studying the time scales of fusion-fission reactions we constructed a code DYNSEQ, which is a time-dependent modification of a simple statistical-model program SEQ [15], coupled with the output of an independent calculation of the nucleus-nucleus dynamics. The program DYNSEQ is a Monte Carlo code that gives the event-averaged particle multiplicity as a function of time. The code allows neutrons, protons, and all complex particles of  $Z = 1, 2, 3$  (up to  ${}^7\text{Li}$ ) to compete in the evaporation cascade. Since the calculation simulates events in which the composite system inevitably undergoes fission ( $P_f = 1$ ), the evaporation cascade is assumed to proceed *during* the dynamic process of fission and therefore the fission width is formally removed from the competition.

It is very important that DYNSEQ is provided “on line” with the actual value of the excitation energy calculated with HICOL. Due to this, the uncertainties associated with the dynamics of the nucleus-nucleus collision and subsequent evolution of the composite system are solved automatically. Note that the HICOL program accounts separately for the amount of excitation energy associated with the thermal, deformation, and rotational energy. Therefore the thermal excitation energy can be directly given as an input to DYNSEQ.

At each stage of the decay cascade described by DYNSEQ the actual value of excitation energy is determined by two factors: the  $Q$  value of the preceding decay and the change of the thermal excitation energy due to the dynamical evolution of the composite system. Once the value of the excitation energy is determined at a given stage of the cascade, the actual decay time  $t'$  is sampled assuming the decay rate proportional to  $\exp(-t/\tau)$ , where the mean lifetime  $\tau$  is given by an approximate expression [16, 17] obtained by integrating the Weisskopf formula for the total decay width  $\Gamma_{\text{tot}}$ :

$$\tau = \frac{\hbar}{\Gamma_{\text{tot}}}, \quad (1)$$

$$\Gamma_{\text{tot}} \approx \sum_i \frac{g_i m_i}{\pi^2 \hbar^2} (\pi R^2) \left( \frac{W_i}{a_i} \right) \exp 2(\sqrt{a_i W_i} - \sqrt{a_c E_c^*}). \quad (2)$$

In this expression  $E_c^*$  is the excitation energy of the nucleus before evaporation,  $a_c$  and  $a_i$  are the level density parameters for nuclei before and after evaporation, respectively,  $W_i = E_c^* - S_i - V_i$  is the maximum value of the excitation which the nucleus may possess after evaporating a particle  $i$  ( $S_i$  is the separation energy and  $V_i$  is the Coulomb energy for particle  $i$ ),  $g_i = 2I_i + 1$  is the spin weighting factor, and  $m_i$  is the mass of the particle  $i$ . The  $\pi R^2$  factor is an approximate (geometrical) value of the inverse reaction cross section.

After the decay time  $t'$  has been sampled, the kind of the evaporated particle  $i$  is determined (by sampling the value of  $\sum_{j=1}^i \Gamma_j / \Gamma_{\text{tot}}$ ), and finally the actual kinetic energy of the selected particle is sampled (assuming its energy spectrum of the Maxwell-Boltzmann shape).

Then the next step of the cascade is calculated according to the same prescription with the new value of  $E^*$ : the next decay time  $t''$  is sampled as well as the kind and energy of the particle. The cascade stops when emission of the consecutive particle is energetically impossible. The event-averaged results of such a multicascade calculation give the relations between time and particle multiplicity (accumulated until that time) separately for all kinds of light particles included in the evaporation code.

It should be noted that the way of using the information on the dynamic evolution of the composite system in the statistical code implies that at each instant of time the system is equilibrated in all degrees of freedom except those related to shape deformation. To be consistent with this approach, we introduced a shape-dependent factor that scales the Weisskopf formula proportionally to the surface of the deformed system,  $S_{\text{def}}$ . In this way the variation of the inverse reaction cross section with the deformation,

$$\sigma_{\text{inv}} \approx \pi R^2 \frac{S_{\text{def}}}{4\pi R^2}, \quad (3)$$

has been formally taken into account in Eq. (2) and properly matched to the extreme case of the scission configuration.

### C. Coupling with nuclear dynamics

As mentioned above, all necessary information on the dynamical evolution of the composite system is supplied to the input of our code DYNSEQ from the Feldmeier program HICOL. The HICOL program gives a realistic macroscopic description of nucleus-nucleus collisions, based on the concept of one-body dissipation [18–20, 12]. In Feldmeier's model [11, 12] a nucleus-nucleus collision is considered in the configuration space of three shape variables, similar to those mentioned in Ref. [20] (namely  $\rho$ ,  $\sigma$ , and  $\Delta$ ), that represent, respectively, the distance between geometrical centers of the fragments, the thickness of the “neck” connecting the two fragments, and the asymmetry in their size (or mass). Classical equations of motion with inclusion of one-body dissipation in the form of the “window-plus-wall” formula [18, 12] are solved numerically in the  $(\rho, \sigma, \Delta)$  configuration space assuming the “Yukawa-plus-exponential” potential [21] and the inertia tensor in the Werner-Wheeler approximation to irrotational mass flow. The HICOL code does not contain free parameters and consistently describes dynamical evolution of various composite systems formed in nucleus-nucleus collisions in a wide range of impact parameters.

The importance of the dynamic effects in the statistical-model calculations is demonstrated in Figs. 1 and 2 for two exemplary reactions,  $^{16}\text{O} + ^{197}\text{Au}$  ( $E_{\text{lab}} = 288 \text{ MeV}$ ) and  $^{40}\text{Ar} + ^{238}\text{U}$  ( $E_{\text{lab}} = 249 \text{ MeV}$ ), for which the prescission neutron multiplicities have been measured [4] and used to determine the time scale of the fusion-fission processes. Figures 1 and 2 show predictions of the program HICOL for these reactions. Displayed is the thermal excitation energy  $E_{\text{diss}}$  released in the composite system as a function of time and angular momentum. It is clearly seen that the “nondynamical” approach, represented by the constant (equilibrium) value of the excitation energy,  $E_{\text{eq}}^* = Q_{\text{g.s.}}^{\text{fusion}} + E_{\text{c.m.}}$ , is too simplistic.

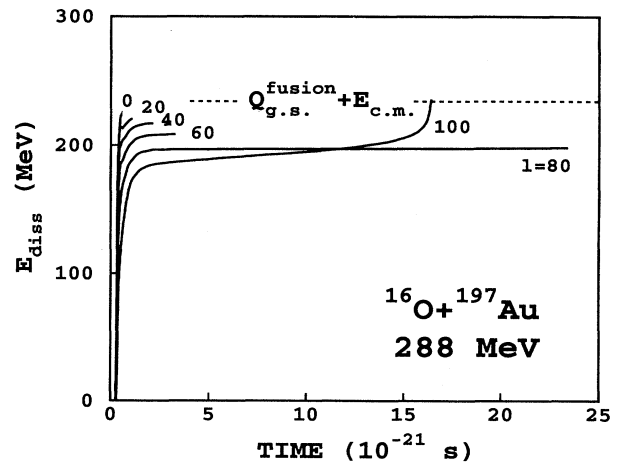


FIG. 1. Thermal excitation energy  $E_{\text{diss}}$ , generated as a function of time in the  $^{16}\text{O} + ^{197}\text{Au}$  reaction at 288 MeV, calculated with the program HICOL for several  $\ell$  values. The equilibrium excitation energy  $E_{\text{eq}}^* = Q_{\text{g.s.}}^{\text{fusion}} + E_{\text{c.m.}}$  is indicated by the dashed line.

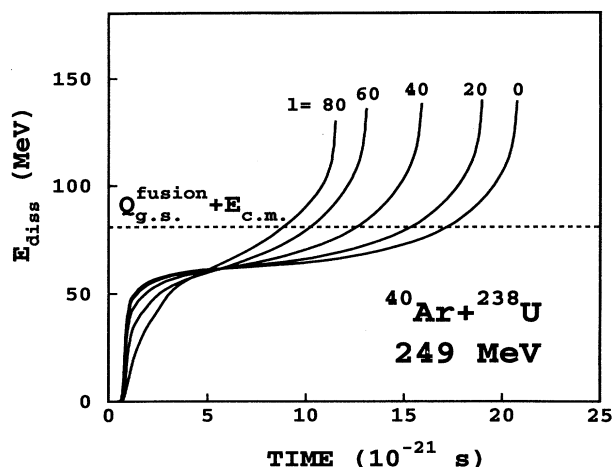


FIG. 2. Same as Fig. 1, except for the  $^{40}\text{Ar} + ^{238}\text{U}$  reaction at 249 MeV.

Figures 1 and 2 show that the equilibrium value of the excitation energy,  $E_{\text{eq}}^*$ , is quickly attained only for the lowest angular momenta and for asymmetric systems, for which Coulomb repulsion is not too strong. But even for the  $^{16}\text{O} + ^{197}\text{Au}$  reaction (see Fig. 1), and a typical fusion trajectory for a nearly central collision at  $\ell = 40$ , the thermal excitation energy,  $E_{\text{diss}}$ , stabilizes some 20 MeV below the equilibrium value. For higher partial waves (still leading to fusion) the deviations from the equilibrium limit are much more severe. Although a large portion of the nonthermal excitation energy,  $E_{\text{eq}}^* - E_{\text{diss}}$ , is “frozen” in rotational degrees of freedom (and thus at least roughly can be accounted for by the static calculation), the effects associated with the shape degrees of freedom are out of the reach of the static model.

Even more dramatic deviations are seen for the  $^{40}\text{Ar} + ^{238}\text{U}$  reaction at 249 MeV (Fig. 2). The HICOL code predicts no fusion in this reaction, even for  $\ell = 0$ . Therefore, most likely, the extracted precission multiplicity in this reaction [4] has to be entirely attributed to fast-fission processes. Since the excitation energy continuously increases throughout the fast-fission process, the analysis of the precission neutron emission in terms of a “static” composite system having the equilibrium excitation energy from the very beginning ( $t = 0$ ) is completely inadequate for this class of reactions.

We performed systematic calculations with the HICOL code for all the systems for which Hinde *et al.* [4] had measured the precission neutron multiplicities and deduced the time scales of the fusion-fission reactions. We found that for the main part of the studied systems, the experimentally observed “fusion-fission” reactions contain a large portion of fast-fission-type processes characterized by the complete damping of the kinetic energy and a nearly symmetric split of mass, occurring for the trajectories which do not surpass the saddle point in the entrance channel. Such a situation is typical for very heavy systems, e.g.,  $^{40}\text{Ar} + ^{238}\text{U}$ , even at low energies, and also for lighter and more asymmetric systems, e.g.,  $^{16}\text{O} + ^{197}\text{Au}$ , at higher energies, above 10 MeV/nucleon.

This is due to the fact that the saddle for heavy systems is located at rather compact “mononuclear” configurations [20, 12].

Consequently, for a wide range of partial waves, the composite system is driven into an almost flat region of the total (nuclear + Coulomb + centrifugal) potential-energy surface. In the absence of a well-defined driving force in that region, HICOL predicts the prolonged rotation of the composite dinuclear system. In the studied [4] reactions, such behavior is predicted for many partial waves. For example, in the  $^{16}\text{O} + ^{197}\text{Au}$  reaction at 288 MeV, the prolonged rotation in the near-saddle configuration (at least two full revolutions) is predicted for all partial waves in the range from  $\ell = 85$  to  $\ell = 120$ .

Of course, the macroscopic, deterministic model is not able to give an exact prediction of how long the dinuclear system (or the deformed mononucleus) will rotate in this metastable configuration with an almost completely vanishing driving force. Such a system will behave in a stochastic way, and therefore its further evolution should be described in terms of the formalism based on the Langevin equation (see, e.g., Refs. [22–24]) rather than in terms of a deterministic model. However, only the macroscopic, deterministic calculations give as yet the possibility to predict the dynamic path in the entrance channel (towards the formation of the “metastable” rotating system), and also the dynamic evolution in the exit channel, i.e., when the system gets well outside the flat landscape of the saddle configuration.

Taking into account the above considerations, we analyze the time scales of fusion-fission reactions by using the scheme of the dynamical evolution of the composite system as shown in Fig. 3. The thermal excitation energy  $E_{\text{diss}}$  is calculated for a given  $\ell$  value with the HICOL code for the whole entrance part of the trajectory—until  $t = t_1$ , when HICOL decides that the system is destined to fuse. The criterion taken for fusion is that either the system surpasses the saddle of the potential-plus-centrifugal energy (usually for relatively light systems and low  $\ell$  values) or that the time limit is exceeded in case of the pro-

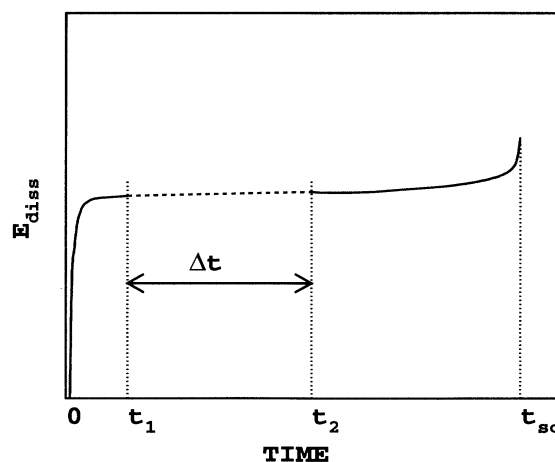


FIG. 3. Schematic illustration of the method of the determination of the time  $\tau_f$  from the measured precission neutron multiplicities  $\nu_{\text{pre}}^{\text{exp}}$ . The interval  $\Delta t$  was adjusted to reach the value  $\nu_{\text{pre}}^{\text{exp}}$  at scission (see text).

longed rotation (for larger  $\ell$  values). HICOL is also used for calculating the final stage of the fusion-fission trajectory, starting at  $t = t_2$  (see Fig. 3) when the composite system is assumed to emerge outside the saddle and move down the fission valley towards scission. Between  $t_1$  and  $t_2$  the composite system remains fused. The transient time  $\Delta t = t_2 - t_1$  is simply left as a parameter that can be determined empirically by fitting the calculated neutron precission multiplicity to the experimental value. Since the amount of the excitation energy dissipated in the composite system during the time between  $t_1$  and  $t_2$  is small, we assume in the calculations that  $E_{\text{diss}}$  can be linearly interpolated (as shown in Fig. 3) in this time interval.

It is important to note that the fast-fission reactions which, as discussed above, contribute to a large (and undistinguishable from fusion-fission) portion of the experimental precission multiplicities, should also be viewed in terms of the scheme presented in Fig. 3. For example, the dynamical evolution of the  $^{16}\text{O} + ^{197}\text{Au}$  system at 288 MeV for  $\ell = 100$  (see Fig. 1) proceeds essentially according to the scheme of Fig. 3, showing a long plateau that reflects the stage of rotation of the metastable dinuclear system. As discussed earlier, the deterministic model cannot reliably predict how long the rotation will last, and therefore, the stretch of the plateau should be left free for an empirical determination, in the same way as for fusion-fission reactions.

Obviously, in the experiments aimed to measure the precission multiplicities it is impossible to distinguish the “true” fusion-fission reactions from fast-fission processes. Therefore, the measured precission neutron multiplicities represent the  $\ell$ -weighted average values covering both the fusion-fission and fast-fission reactions. It is a somewhat arbitrary decision what value of effective angular momentum to choose in our analysis to represent the combined class of fusion-fission and fast-fission reactions. The  $(2\ell + 1)$  factor acts in favor of higher partial waves (i.e., fast-fission reactions). On the other hand, for lower partial waves (i.e., for “true” fusion-fission reactions), the precission multiplicities must be larger, and this should counterbalance the effect of the  $(2\ell + 1)$  factor. In our calculations presented in the next section we consistently used the  $\ell$  value that divides the fusion-fission reactions from the fast-fission processes (i.e., the critical angular momentum predicted by the program HICOL) as representing the average dynamical behavior of the system.

At the end of this section we would like to make a brief comment on the work of Aleshin [25] who applied similar techniques (the combination of an evaporation code with the dynamics of the composite system) for calculating light particle emission in dissipative collisions. Conceptually, the model of Aleshin cannot describe “true” fusion-fission reactions and is equivalent to our model in the  $\Delta t = 0$  limit. Unfortunately, as discussed above, the existing data always represent an unseparable mixture of “true” fusion-fission and fast-fission reactions. Therefore comparisons of predictions of the model [25] with the measured precission neutron multiplicities seem to be unjustified.

### III. RESULTS OF CALCULATIONS AND DISCUSSION

We performed our calculations for the complete set of data on precission neutron multiplicities measured and compiled by Hinde *et al.* in Ref. [4]. The results are presented in Table I. The listed reactions comprise compound systems of the combined atomic number ranging from  $Z = 55$  ( $^{16}\text{O} + \text{Ag}$ ) to  $Z = 120$  ( $^{64}\text{Ni} + ^{238}\text{U}$ ). To give approximate information on the magnitude of the excitation energies generated in these composite systems, Table I lists  $E_{\text{eq}}^* = Q_{\text{g.s.}}^{\text{fusion}} + E_{\text{c.m.}}$ , corresponding to the excitation energy of the fully equilibrated compound nuclei (prior to particle emission). These  $E_{\text{eq}}^*$  values range from 80 to 240 MeV.

The method of determining  $\tau_f$  values (listed in the last column of Table I) from the precission neutron multiplicities is illustrated in Fig. 4, taking the  $^{16}\text{O} + ^{197}\text{Au}$  reaction at 288 MeV as an example. The line labeled  $E_{\text{diss}}$  (in the upper part of Fig. 4) shows the growth of the dissipated energy  $E_{\text{diss}}$ , predicted for the entrance and exit parts of the trajectory by the code HICOL for  $\ell = \ell_{\text{cr}} = 82$ . The line below (labeled  $E^*$ ) represents the development in time of the actual excitation energy,  $E^*$ , that is the net result of the gradual generation of the excitation energy,  $E_{\text{diss}}(t)$ , and successive deexcitation due to particle evaporation calculated with the code DYNSEQ.

The lower part of Fig. 4 shows the accumulation in time of the neutron multiplicity  $\nu_{\text{pre}}(t)$ . The value of  $\tau_f$  is determined by the crossing of  $\nu_{\text{pre}}(t)$  with the dashed line at the level of the measured multiplicity  $\nu_{\text{pre}}^{\text{exp}}$ .

Calculations of  $\nu_{\text{pre}}(t)$  for all reactions listed in Table

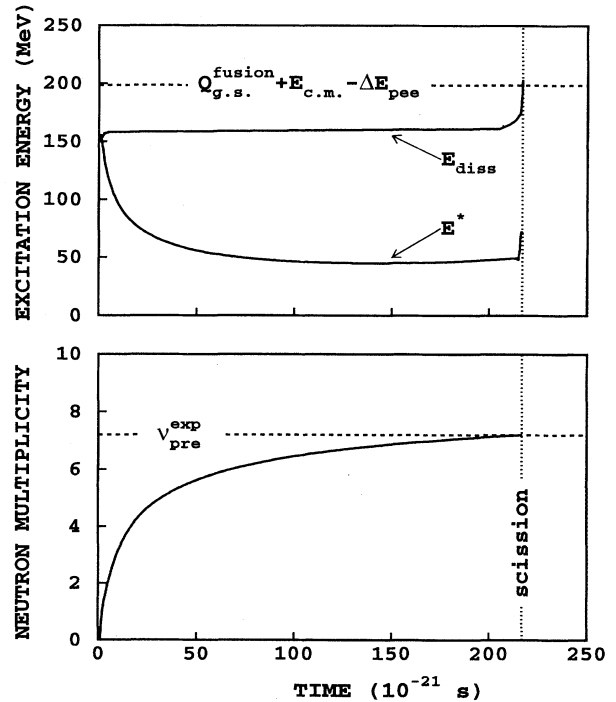


FIG. 4. Example of the determination of the fusion-fission time  $\tau_f$  in the  $^{16}\text{O} + ^{197}\text{Au}$  reaction at 288 MeV. For explanations see text.

TABLE I. Values of the fusion-fission time scale,  $\tau_f$ , deduced from experimentally determined precession neutron multiplicities  $\nu_{\text{pre}}$ . All the values of  $\nu_{\text{pre}}$  and estimated energies removed by preequilibrium nucleons,  $\Delta E_{\text{pee}}$ , are taken from Ref. [4]. The critical angular momenta for fusion,  $\ell_f$ , are calculated with the code HICOL.

Reaction	$E_{\text{lab}}$ (MeV)	$E_{\text{eq}}^*$ (MeV)	$\Delta E_{\text{pee}}$ (MeV)	$\nu_{\text{pre}}$	$\ell_f$	$\tau_f$ ( $10^{-21}$ s)
$^{18}\text{O} + ^{238}\text{U}$	158.8	109.3	3.1	$5.10 \pm 0.25$	57	$340 \pm_{50}^{80}$
$^{18}\text{O} + ^{197}\text{Au}$	158.8	113.3	3.2	$4.10 \pm 0.15$	73	$300 \pm_{60}^{70}$
$^{18}\text{O} + ^{169}\text{Tm}$	158.8	121.2	4.7	$3.70 \pm 0.30$	81	$410 \pm_{170}^{400}$
$^{18}\text{O} + ^{154}\text{Sm}$	158.8	128.2	5.7	$4.40 \pm 0.15$	82	$540 \pm_{150}^{200}$
$^{18}\text{O} + ^{144}\text{Sm}$	158.8	118.4	4.2	$2.45 \pm 0.25$	76	$220 \pm_{40}^{110}$
$^{18}\text{O} + ^{124}\text{Sn}$	158.8	134.2	6.8	$2.90 \pm 0.25$	79	$53 \pm_{15}^{20}$
$^{16}\text{O} + ^{238}\text{U}$	288.0	231.5	34.7	$9.0 \pm 0.5$	66	$70 \pm_{20}^{30}$
$^{16}\text{O} + ^{208}\text{Pb}$	288.0	220.9	31.7	$6.9 \pm 0.3$	81	$33 \pm_{5}^{14}$
$^{16}\text{O} + ^{197}\text{Au}$	288.0	234.0	35.5	$7.2 \pm 0.2$	82	$220 \pm_{40}^{70}$
$^{16}\text{O} + ^{184}\text{W}$	288.0	240.9	37.5	$7.7 \pm 0.3$	87	$210 \pm_{60}^{100}$
$^{16}\text{O} + ^{154}\text{Sm}$	288.0	244.5	43.0	$8.4 \pm 0.4$	97	$2200 \pm_{1500}^{8000}$
$^{16}\text{O} + ^{109}\text{Ag}$	288.0	237.2	49.2	$4.0 \pm 0.5$	90	$470 \pm_{350}^{3000}$
$^{40}\text{Ar} + ^{238}\text{U}$	249.0	80.9		$3.25 \pm 0.20$	0 <sup>a</sup>	$390 \pm_{60}^{80}$
$^{40}\text{Ar} + ^{208}\text{Pb}$	249.0	80.1		$2.00 \pm 0.15$	34 <sup>a</sup>	$130 \pm_{15}^{15}$
$^{40}\text{Ar} + ^{197}\text{Au}$	249.0	86.8		$2.95 \pm 0.30$	44	$190 \pm_{50}^{80}$
$^{40}\text{Ar} + ^{181}\text{Ta}$	249.0	98.1		$3.68 \pm 0.28$	61	$620 \pm_{220}^{600}$
$^{40}\text{Ar} + ^{169}\text{Tm}$	249.0	108.9		$3.00 \pm 0.30$	69	$510 \pm_{200}^{400}$
$^{40}\text{Ar} + ^{165}\text{Ho}$	249.0	113.6		$2.85 \pm 0.30$	74	$350 \pm_{140}^{260}$
$^{40}\text{Ar} + ^{141}\text{Pr}$	249.0	112.7		$2.65 \pm 0.30$	85	$800 \pm_{450}^{900}$
$^{64}\text{Ni} + ^{238}\text{U}$	417.7	88.8		$4.00 \pm 0.80$	0 <sup>a</sup>	$120 \pm_{40}^{90}$
$^{64}\text{Ni} + ^{208}\text{Pb}$	417.7	94.3		$3.25 \pm 0.60$	0 <sup>a</sup>	$70 \pm_{25}^{35}$
$^{64}\text{Ni} + ^{197}\text{Au}$	417.7	102.2		$3.15 \pm 0.60$	0 <sup>a</sup>	$80 \pm_{25}^{55}$
$^{64}\text{Ni} + ^{175}\text{Lu}$	417.7	119.0		$3.30 \pm 0.50$	14 <sup>a</sup>	$45 \pm_{15}^{30}$
$^{64}\text{Ni} + ^{154}\text{Sm}$	417.7	143.2		$3.90 \pm 0.35$	60	$65 \pm_{20}^{30}$

<sup>a</sup> For all the reactions for which  $\ell_f < 40$  the time scale  $\tau_f$  was calculated for  $\ell = 40$ .

I were made for a value of the level density parameter  $a = A/10$ . Using the example reaction  $^{16}\text{O} + ^{197}\text{Au}$ , illustrated in Fig. 4, we checked that for rational values of  $a$  ranging from  $A/13$  to  $A/8$  the deduced time scale  $\tau_f$  varies from  $200 \times 10^{-21}$  to  $280 \times 10^{-21}$  s. (Sensitivity of the deduced time scale to the level density parameter decreases with the multiplicity.) Also for other systems the variation of  $a$  leads to an effect of similar magnitude that as a rule is smaller than the uncertainty in determination of  $\tau_f$  associated with the inaccuracy of the  $\nu_{\text{pre}}^{\text{exp}}$  value.

Figure 5 presents calculations for the same system as in Fig. 4, but in the “static” approach. In the static version the full value of the compound-nucleus excitation energy,  $E_{\text{eq}}^*$ , is available for the evaporation cascade right from the beginning, at  $t = 0$ . Therefore the calculated rate of the cascade is faster and the value  $\nu_{\text{pre}}^{\text{exp}}$  is reached earlier.

The difference in the deduced time scales of the dynamic and static approaches, presented in Figs. 4 and 5, is characteristic for all the systems interpreted by Hinde *et al.* [4] (static calculations) and in this work. The time scales deduced in Ref. [4] are even shorter than those calculated in our “static” version exemplified by Fig. 5 because Hinde and co-workers used as the input excitation energy the value of  $E^* = E_{\text{eq}}^* + \Delta E_x$ , where  $\Delta E_x$  for heavy systems ( $A > 200$ ) was assumed to be positive. ( $\Delta E_x$  can be interpreted as the amount of energy released and equilibrated on the way from saddle to scis-

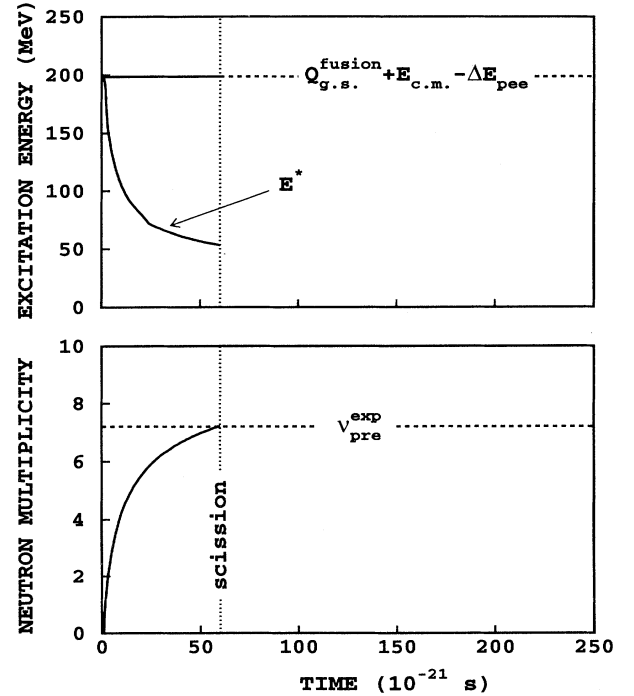


FIG. 5. Same as Fig. 4, except for the “static” approach. The value  $\nu_{\text{pre}}^{\text{exp}}$  is reached in a considerably shorter time than in the realistic (dynamic) calculation presented in Fig. 4.

sion.) As it is seen from the dynamic calculations (see Figs. 1, 2, and 4), the additional excitation energy that might be related to  $\Delta E_x$  is generated in the last stage of fission (in about  $10^{-21}$  s just before scission) and therefore it has practically no influence on the final value of  $\nu_{\text{pre}}$ .

It is seen from Fig. 4 that the accumulation of  $\nu_{\text{pre}}$  in time is by far not linear. It almost saturates after some time and therefore experimental errors in determination of  $\nu_{\text{pre}}^{\text{exp}}$  result in much larger relative uncertainties of the deduced time scale  $\tau_f$  (see Table I). As discussed in Sec. II C, an additional uncertainty is associated with the choice of an effective average value of the angular momentum in DYNSEQ calculations. The role of this factor is illustrated in Fig. 6, again with the  $^{16}\text{O} + ^{197}\text{Au}$  reaction at 288 MeV used as an example. It is seen from Fig. 6 that realistic assumptions concerning the effective  $\ell$  value lead to rather small uncertainties in the determination of  $\tau_f$  in comparison with those resulting from the experimental errors of the precession multiplicities.

It is interesting to note that within the large errors, the  $\tau_f$  values do not show any specific trend or dependence on the excitation energy. As shown in Fig. 7, the studied reactions are clustered into two regions of  $E_{\text{eq}}^*$ . Although the deduced  $\tau_f$  values are very dispersed within each of the two regions, any realistic interpolation between low and high excitation energies excludes a clear dependence of  $\tau_f$  on  $E_{\text{eq}}^*$ .

In Fig. 8 the complete set of the deduced  $\tau_f$  values is displayed as a function of the combined mass number of the colliding system,  $A = A_1 + A_2$ . Results of the analysis of Hinde *et al.* (in the static approach) are also shown for comparison. It is seen that our dynamic calculations systematically result in a significantly longer time scale  $\tau_f$  (on average, by a factor of 10). We have checked that the statistical cascade code used in our analysis (SEQ) and that in Ref. [4] (JULIAN) give practically identical results for equivalent initial conditions. Therefore, the difference between our results and those of Ref. [4], presented in Fig. 8, originates entirely from the difference

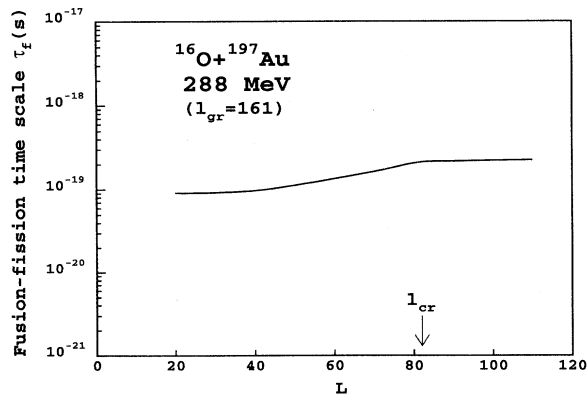


FIG. 6. The fusion-fission time  $\tau_f$  in the  $^{16}\text{O} + ^{197}\text{Au}$  reaction at 288 MeV, deduced from the measured precession neutron multiplicity, plotted as a function of an assumed value of the effective (average) angular momentum  $L$  representing the entire range of the observed fusion-fission-like reactions.

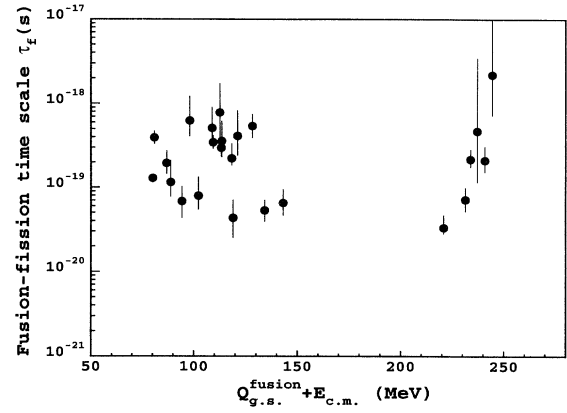


FIG. 7. Fusion-fission time scale  $\tau_f$  for all reactions analyzed in this work, plotted as a function of the quantity  $E_{\text{eq}}^* = Q_{\text{g.s.}}^{\text{fusion}} + E_{\text{c.m.}}$ .

in treating the dynamics of the fusion-fission reactions. Similar to the static analysis [4], the  $\tau_f$  values deduced in the present work show a trend of decreasing value with increasing mass of the composite system.

Summing up the method of our analysis, we would like to make clear that the deduced  $\tau_f$  values represent the total duration of the fusion-fission process: from touching spheres ( $t = 0$ ) to fusion or formation of a mononucleus ( $t = t_1$ ), then to the saddle ( $t = t_2$ ), and finally to scission ( $t = t_{\text{sc}}$ ), as shown in Fig. 3. Our analysis shows that the major contribution to  $\tau_f$  comes from the intermediate stage,  $\Delta t = t_2 - t_1$ . As it was pointed out in Sec. II C, duration of that stage cannot be predicted by a deterministic classical model. Therefore for each particular reaction  $\Delta t$  is deduced “empirically” by using the neutron clock.

For all studied reactions, both the time required to reach fusion (or to form a mononucleus),  $t_1$ , and the saddle-to-scission time,  $t_{\text{sc}} - t_2$ , turn out to be short in

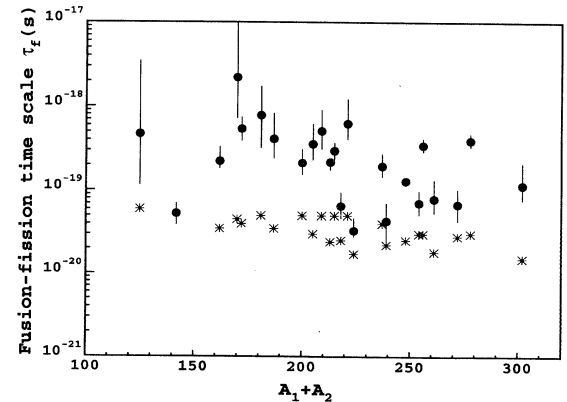


FIG. 8. Fusion-fission time scale  $\tau_f$  for all reactions analyzed in this work (solid circles), plotted as a function of the combined mass number of the system,  $A_1 + A_2$ . The asterisks show the  $\tau_f$  values deduced with the static model of Ref. [4].

comparison with the total time  $\tau_f$ . Typically,  $t_1/\tau_f = 0.01 - 0.1$  and  $(t_{sc} - t_2)/\tau_f$  ranges from 0.05 to at most 0.5. Therefore the long fusion-fission times  $\tau_f$  have to be primarily associated with the intermediate stage of the composite system.

It should be noted here that the long fusion-fission times  $\tau_f$ , obtained in our analysis of the prescission neutron multiplicities, agree with results of conceptually different analysis of the prescission GDR  $\gamma$  multiplicities reported in Ref. [10]. As mentioned in Sec. II A, in the model used by Paul and Thoennessen [10] the compound-nucleus fission time (denoted in the present work by  $\Delta t$ ) can be related to the value of the dissipation coefficient. Therefore, similar to the fission times deduced from the GDR data, the very long fusion-fission times  $\tau_f$  found in our analysis of the prescission neutron multiplicities can also be interpreted (in terms of the model [10]) as evidence of an unexpectedly large value of the dissipation coefficient in hot composite systems.

Summarizing, we analyzed existing data on the prescission neutron multiplicities in terms of a new method combining the time-dependent statistical-model calculations with the dynamical description of the composite system. Results of the present analysis show that independently of the mass or excitation energy of the composite system, the process of its binary division into comparable fragments (i.e., fission and/or “fast-fission”) requires quite a long time, on the order of  $10^{-19}$  s. This time interval

can be interpreted (classically) as the time needed for the considerable collective rearrangement of the system, or (in the language of quantum mechanics) as manifestation of a small value of the matrix element representing the transition from the compound nucleus to the scission configuration.

We demonstrated that a realistic inclusion of the dynamics of the fusion-fission reactions leads to much longer  $\tau_f$  values than those predicted by “static” calculations [4, 26]. The deduced time scales typically range from  $5 \times 10^{-20}$  to  $10^{-18}$  s, whereas results of the static calculations [4] range from  $2 \times 10^{-20}$  to  $5 \times 10^{-20}$  s. Much longer time scales of the fusion-fission reactions deduced in our dynamic approach show that the measurements of the prescission and postscission neutron multiplicities represent a sensitive tool for studying the dynamics of nucleus-nucleus collisions.

### ACKNOWLEDGMENTS

The authors would like to thank Hans Feldmeier for providing us with the program HICOL. This work was performed as a part of the research program of the Committee of Scientific Research of Poland (KBN Grant No. 2P302-211-04) and the Stichting voor Fundamenteel Onderzoek der Materie (FOM) with financial support of the Nederlandse Organisatie voor Wetenschappelijk Onderzoek (NWO).

- [1] A. Gavron, J.R. Beene, B. Cheynis, R.L. Ferguson, F.E. Obenshain, F. Plasil, G.R. Young, G.A. Petitt, M. Jääskeläinen, D.G. Sarantites, and C.F. Maguire, *Phys. Rev. Lett.* **47**, 1255 (1981).
- [2] E. Holub, D. Hilscher, G. Ingold, U. Jahnke, H. Orf, and H. Rossner, *Phys. Rev. C* **28**, 252 (1983).
- [3] D. Ward, R.J. Charity, D.J. Hinde, J.R. Leigh, and J.O. Newton, *Nucl. Phys.* **A403**, 189 (1983).
- [4] D.J. Hinde, D. Hilscher, H. Rossner, B. Gebauer, M. Lehmann, and M. Wilpert, *Phys. Rev. C* **45**, 1229 (1992).
- [5] D.J. Hinde, in *Proceedings of the International Nuclear Physics Conference*, Wiesbaden, Germany, 1992, edited by R. Bock, H. Emling, E. Grosse, U. Grundinger, K.D. Hildebrand, and J. Knoll [*Nucl. Phys.* **A553**, 255c (1993)].
- [6] E. Duek, N.N. Ajitanand, J.M. Alexander, D. Logan, M. Kildir, L. Kowalski, L.C. Vaz, D. Guerreau, M. S. Zisman, M. Kaplan, and D.J. Moses, *Z. Phys. A* **317**, 83 (1984).
- [7] B. Lindl, A. Bruckner, M. Bantel, H. Ho, R. Muffler, L. Schad, M.G. Trauth, and J.P. Wurm, *Z. Phys. A* **328**, 85 (1987).
- [8] K. Siwek-Wilczyńska, J. Wilczyński, H.K.W. Leegte, R.H. Siemssen, H.W. Wilschut, K. Grotowski, A. Panasiewicz, Z. Sosin, and A. Wieloch, *Phys. Rev. C* **48**, 228 (1993).
- [9] J.P. Lestone, J.R. Leigh, J.O. Newton, D.J. Hinde, J.X. Wei, J.X. Chen, S. Elfström, and M. Zielinska-Pfabé, *Nucl. Phys.* **A559**, 277 (1993).
- [10] P. Paul and M. Thoennessen, *Ann. Rev. Nucl. Part. Sci.* **44**, 65 (1994).
- [11] H. Feldmeier, in *Nuclear Structure and Heavy Ion Dynamics*, Proceedings of the International School of Physics “Enrico Fermi,” Course LXXXVII, Varenna, 1982, edited by L. Moretto and R.A. Ricci (North-Holland, Amsterdam, 1984), p. 274.
- [12] H. Feldmeier, *Rep. Prog. Phys.* **50**, 915 (1987).
- [13] N. Bohr and J.A. Wheeler, *Phys. Rev.* **56**, 426 (1939).
- [14] H.A. Kramers, *Physica* **7**, 284 (1940).
- [15] H.W. Wilschut (unpublished).
- [16] K.J. LeCouteur, *Proc. Phys. Soc.* **63A**, 259 (1950).
- [17] K. Kikuchi and M. Kawai, in *Nuclear Matter and Nuclear Reactions* (North-Holland, Amsterdam, 1968).
- [18] J. Blocki, Y. Boneh, J.R. Nix, J. Randrup, M. Robel, A.J. Sierk, and W.J. Swiatecki, *Ann. Phys. (N.Y.)* **113**, 330 (1978).
- [19] J. Randrup, *Nucl. Phys.* **A327**, 490 (1979).
- [20] W.J. Swiatecki, in *Proceedings of the International Conference on Theoretical Approaches of Heavy Ion Reaction Mechanisms*, Paris, 1984, edited by M. Martinot, C. Ngô, and F. Lapage [*Nucl. Phys.* **A428**, 199c (1984)].
- [21] H.J. Krappe, J.R. Nix, and A.J. Sierk, *Phys. Rev. C* **20**, 992 (1979).
- [22] Y. Abe, C. Grégoire, and H. Delagrange, *J. Phys. (Paris)* **47**, C4-329 (1986).
- [23] T. Wada, N. Carjan, and Y. Abe, in *Proceedings of the Fourth International Conference on Nucleus-Nucleus Collisions*, Kanazawa, Japan, 1991, edited by H. Toki, I. Tanihata, and H. Kamitsubo [*Nucl. Phys.* **A538**, 283c (1992)].
- [24] G.R. Tillack, R. Reif, A. Schülke, P. Fröbrich, H.J. Krappe, and H.G. Reusch, *Phys. Lett. B* **296**, 296 (1992).
- [25] V.P. Aleshin, *J. Phys. G* **19**, 307 (1993).
- [26] A. Saxena, A. Chatterjee, R. K. Choudhury, S. S. Kapoor, and D. M. Nadkarni, *Phys. Rev. C* **49**, 932 (1994).